JOURNAL OF APPLIED ELECTROCHEMISTRY 19 (1989) 807-812

Electrochemical studies on solid state cells with mol % $70AgI{-}20Ag_2O{-}10(0.8V_2O_5{-}0.2P_2O_5)$ amorphous electrolyte and organic cathodes

P. SATHYA SAINATH PRASAD, S. RADHAKRISHNA

Department of Physics, Indian Institute of Technology, Madras-600 036, India

Received 21 June 1988; revised 27 November 1988

The highest conducting amorphous solid electrolyte composition (mol %) $70AgI{-}20Ag_2O{-}10(0.8V_2O_5{-}0.2P_2O_5)$ in the system $AgI{-}Ag_2O{-}V_2O_5{-}P_2O_5$ was investigated as an electrolyte material for solid state cells with organic cathodes by studying the electrochemical properties. The variation of open circuit voltage (OCV) with temperature, current discharge and the load characteristics were determined for the cells with iodine, tetramethyl ammonium iodide and tetrabutyl ammonium iodide as cathode materials. The cell capacities were estimated from the load characteristic curves and, in general, the cells were found to have very good stability at low current discharges even at high temperatures. In addition, it was found that the silver on the working electrode is electrochemically active and can be oxidized to Ag^+ ions, making the organic cathode cells rechargeable. Thus these cells find potential use in rechargeable micropower sources and uninterrupted power supplies for microelectronic circuit devices.

1. Introduction

Standard electrochemical cells with solution electrolytes have disadvantages such as corrosion of electrodes with electrolytic solution, leakage of the electrolyte, which leads to limited shelf-life, less ruggedness and narrow temperature range of operation. Electrochemical cells with solid electrolytes having ionic conductivities of the same order of solution electrolytes have improved upon these disadvantages [1-4]. A large number of good solid electrolytes have been developed and extensively used in both low and high energy density batteries [5, 6]. Many polycrystalline materials, especially $RbAg_4I_5$, being the highest ionic conducting material among the silver superionic conducting category, have been developed for micropower sources and their discharge and polarization phenomena have been reported [7-9]. But these batteries based on polycrystalline electrolytes have disadvantages such as diffusion of cathode material into the electrolyte, corrosion of electrode–electrolyte interface, formation of voids and growth of dendrites.

Therefore, research activity has been diverted to amorphous electrolytes with very high ionic conductivity of the order of 10^{-2} $(\mathrm{ohm\,cm})^{-1}$ and an electronic conductivity less than 10^{-8} $(\mathrm{ohm\,cm})^{-1}$ in order to limit the internal shorting current to less than $1.0\,\mu A$ for an average cell. Many amorphous electrolytes based on the Ag^+ ion as conducting species were reported [10] to have an electronic conductivity of 10^{-6} $(\mathrm{ohm\,cm})^{-1}$ which leads to self discharge of a battery and hence a lower shelf-life. So, efforts are being channelled to the search of new amorphous electrolytes to achieve relatively long shelf-life and constant current discharge, when used in solid state batteries.

Thus, in a systematic study, the quaternary superionic conducting system $AgI{-}Ag_2O{-}V_2O_5{-}P_2O_5$ has been investigated and the transport and dielectric properties have been established for $xAgI{-}(1-x)[yAg_2O{-}z(pV_2O_5{-}qP_2O_5)]$ where $50 < x < 80$ mol %, $z/y = 0.2{-}5.0$ and $0.1 < p/q < 0.9$ [11-13]. It was reported that the composition (mol %) $70AgI{-}20Ag_2O{-}10(0.8V_2O_5{-}0.2P_2O_5)$ has the highest ionic conductivity of 8.2×10^{-2} $(\mathrm{ohm\,cm})^{-1}$ and an electronic conductivity of 2.6×10^{-8} $(\mathrm{ohm\,cm})^{-1}$ at 303 K [14]. The glasses were found to be quite stable for long periods. This material displays all the required qualities of a good solid electrolyte and a preliminary investigation was undertaken by using this electrolyte in Ag/I_2 batteries [12]. A study on the electrochemical behaviour of the cells and attempts to improve discharge efficiencies by using tetra-alkyl ammonium iodides in cathode structure are reported in the present communication.

2. Experimental details

2.1. *Preparation and characterization of electrolyte material*

Analar grade chemicals AgI, Ag_2O, V_2O_5 and P_2O_5 were taken in appropriate quantities corresponding to the composition (mol %) $70AgI{-}20Ag_2O{-}10(0.8V_2O_5{-}0.2P_2O_5)$ and thoroughly mixed. The mixture was put into a quartz crucible and melted at 600° C. The homogeneous melt was rapidly quenched onto copper plates maintained at liquid nitrogen temperature.

The same thermal history and quenching rate were maintained for each preparation. Samples were crushed to fine powder and X-ray diffractograms were recorded. The featureless diffractogram obtained has confirmed the absence of crystallinity and the amorphous nature of the sample.

2.2. *Ionic and electronic conductivities*

Ionic conductivity measurements were undertaken on samples pressed together with an electrode mixture of silver powder and electrolyte (1 : 1 ratio by weight) under a pressure of 5000 kg cm^{-2} using a Perkin–Elmer hand press. The purpose of adding electrolyte to electrodes is to minimize the contact resistance between electrode and electrolyte by making reversible electrodes. Resistance measurements were carried out in the temperature range 303–383 K using an impedance bridge GR 1650 B.

For electronic conductivity experiments, Wagner's d.c. polarization technique [15] was adopted for which a pellet of configuration (– Ag)/(electrolyte)/(C+) was made, graphite being a blocking electrode. The steady state current responses were noted for each applied potential less than the decomposition potential of the electrolyte.

2.3. *Electrochemical cells*

2.3.1. Anode. Since the Ag$^+$ ion is the current-carrying species in the electrolyte, polarographic grade silver powder was mixed with finely crushed electrolyte powder in 2 : 1 ratio by weight. To minimize anode–electrolyte interfacial contact resistance, amalgamated silver powder anodes were also employed. Anode powder and 0.2 g of electrolyte powder were pressed together as two separate layers under a pressure of 5000 kg cm^{-2}, resulting in pellets of 1.2 cm diameter.

2.3.2. Cathodes. The cathode material was prepared by mixing iodine granules, electrolyte powder and graphite powder in 5 : 5 : 1 ratio by weight. The cathodes employing tetra-alkyl ammonium iodides were prepared as described by Owens [16]. A mixture was prepared by blending tetra-alkyl ammonium iodide (alkyl = methyl and butyl) and molecular iodine granules in a 1 : 4 ratio and heating slowly up to 120° C in evacuated and sealed glass ampoules. The ampoules were slowly cooled down to room temperature. The finely ground powder of the obtained compounds of the type R_4NI_9 (R = methyl and butyl) was pressed along with graphite and electrolyte powders in 5 : 1 : 5 ratio, into pellets of 1.2 cm diameter.

2.3.3. Cell composition. On a trial and error basis, with different weight ratios of anode, cathode and electrolyte, the best discharge efficiency was obtained for the weight ratios 0.20 g of silver powder, 0.10 g of electrolyte as anode; 1.0 g of electrolyte and 0.5 g of organic cathode material with 0.5 g of electrolyte, 0.1 g of graphite as cathode.

The anode–electrolyte pellet and cathode pellet were pressed together between two ebonite plates and sealed with epoxy resin. So, cells of the following type

$$(\mathrm{Ag})/(\mathrm{electrolyte})/(\mathrm{I_2} + \mathrm{C}) \qquad (\mathrm{I})$$
$$(\mathrm{Ag})/(\mathrm{electrolyte})/(\mathrm{I_2} + \mathrm{TMAI} + \mathrm{C}) \qquad (\mathrm{II})$$
$$(\mathrm{Ag})/(\mathrm{electrolyte})/(\mathrm{I_2} + \mathrm{TBAI} + \mathrm{C}) \qquad (\mathrm{III})$$

were constructed and characterized by studying their open circuit voltages, polarization and discharge profiles.

3. Results and discussion

3.1. *Ionic and electronic conductivities*

The ionic conductivity was found to be 8.2 × 10^{-2} (ohm cm)$^{-1}$ at 303 K with a glass transition temperature of 72° C from the variation of ionic conductivity with temperature plots, above which the ionic conductivity was observed to decrease. This might be due to the nucleation of crystals and slow decomposition of the electrolyte into poorly conducting compounds [17].

In the electronic conductivity experiment, the observed current response (I_e) seem to be saturating at higher applied potential, which indicates the absence of electronic-hole current. The value of the electronic conductivity was calculated from the formula

$$\sigma_e = (RTA/LF)$$

where L and A are the thickness and area of the polarization cell, R is the universal gas constant, F is the Faraday constant and T is the absolute temperature. σ_e was found to be 2.6 × 10^{-8} (ohm cm)$^{-1}$ at 303 K.

From the ionic and electronic conductivities, the transport numbers of silver ions and electrons were calculated to be 0.9999 and 0.0001 respectively which indicates the suitability of the electrolyte for battery applications.

3.2. *Open circuit voltage*

The open circuit voltage (OCV) of cells of type I, II and III measured with a high impedance digital microvoltmeter were 682, 640 and 630 mV, respectively. The low open circuit voltages for cells using organic cathodes (TMAI and TBAI), when compared to the cells with I_2 cathodes, were due to the different energy of formation of the cell reactions. In the pure I_2 cathode cells, the cell reaction is

$$\mathrm{Ag} + 1/2\ \mathrm{I_2} \longrightarrow \mathrm{AgI}$$

whereas in organic cathode cells, it is speculated as

$$\mathrm{Ag} + 1/2(\mathrm{I_2\text{-}TBAI}) \longrightarrow \mathrm{AgI} + 1/2\ \mathrm{TBAI\ complex}$$

The theoretical calculations from the thermodynamic studies to determine the exact energy of formation of these reactions are yet to be undertaken. The decrease

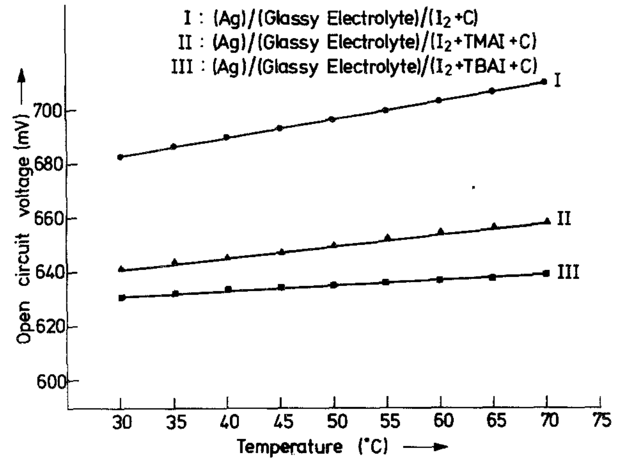

Fig. 1. The variation of open circuit voltage (OCV) with temperature for the amorphous electrolyte material (mol %) 70AgI–$20Ag_2O$–$10(0.8V_2O_5$–$0.2P_2O_5)$ with iodine (1), tetramethyl ammonium iodide (2) and tetrabutyl ammonium iodide (3) cathodes.

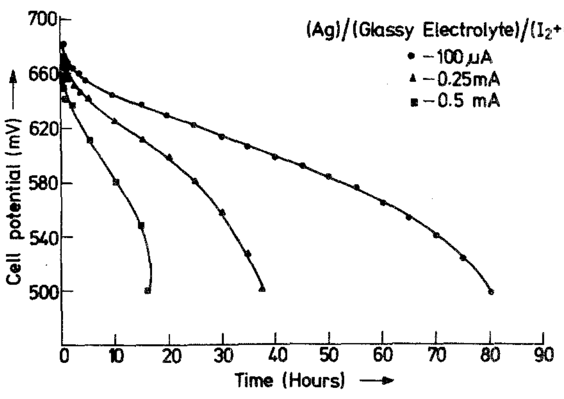

Fig. 2. The current discharge profile curves of the amorphous electrolyte cell (Ag)/(electrolyte)/(I_2 + C) at different current drains of 100 μA (●), 0.25 mA (▲) and 0.5 mA (■).

in OCV from methyl to butyl indicates that the alkyl group in the cathode affects the cathode reduction potential. From these experimental observations, and as suggested by Scrosati *et al.* [18], it can be concluded that, as the alkyl group increases, it traps molecular iodine, thus reducing its activity for the cell reaction as explained above.

The OCV values of the present investigation were comparatively high compared with those reported by Owens [19] in the case of (Ag + Hg)/($RbAg_4I_5$)/(TBAI). The low values reported by Owens might be due to amalgamation of the silver anode which reduces the Ag^+ ion activity and mobility when compared to a pure silver anode. The decrease in OCV from methyl to butyl indicates that the alkyl group in the cathode affects the cathode reduction potential. The OCV values of cells of types II and III did not vary during a 3-month storage period at room temperature, suggesting that the iodine diffusion did not occur through the electrolyte. The variation of OCV with temperature is shown in Fig. 1 The lesser values of OCV and less dependence on temperature for cells of types II and III indicates the reduced iodine activity in the cathode material which leads to longer shelf-life of a battery.

The transport number of silver ions and electrons were calculated by considering the ratio of the observed open circuit voltage and the theoretical value of 687.0 mV reported for the Ag/I_2 couple from thermodynamic studies [5]. The transport numbers of silver ions and electrons were found to be 0.992 and 0.007 respectively for cell I and compare well with the values calculated from conductivity studies. The observed lower values of the silver ion transport number for cells II and III confirm the reduced iodine activity in the presence of tetra-alkyl ammonium iodides.

3.3. *Discharge characteristics*

Figures 2, 3 and 4 indicate the discharge profiles of cells I, II and III respectively at various current drains discharged up to 500 mV.

In Fig. 2 the discharge efficiency seems to be greater only at low discharge currents. The initial drop in cell potential in the first few hours is due to the formation of low-conducting AgI compound at the cathode–electrolyte interface. The observation of an approximately tenfold increase in the internal resistance over the initial value of the cell, after the discharge process is completed, also confirms the formation of high resistive layers of AgI at the cathode–electrolyte interface.

Figures 3 and 4 show the discharge profiles for

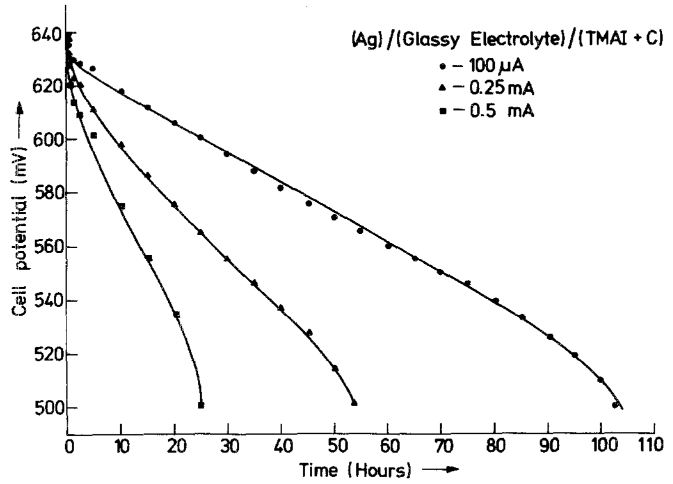

Fig. 3. The current discharge profile curves of the amorphous electrolyte cell (Ag)/(electrolyte) (I_2 + TMAI + C) at different current drains of 100 μA (●), 0.25 mA (▲) and 0.5 mA (■).

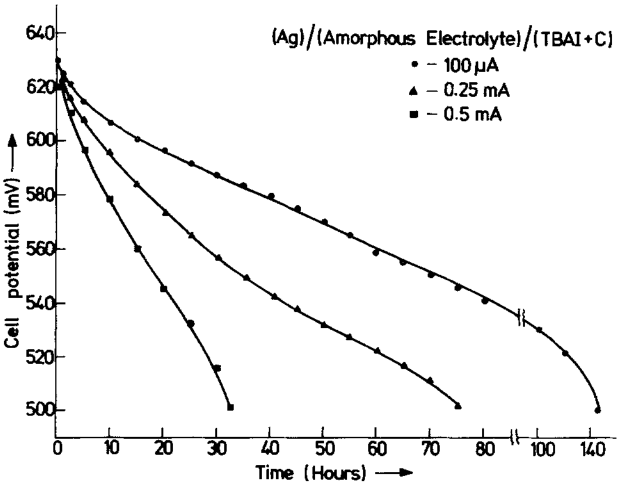

Fig. 4. The current discharge profile curves of the amorphous electrolyte cell (Ag)/(electrolyte) (I_2 + TBAI + C) at different current drains of 100 μA (●), 0.25 mA (▲) and 0.5 mA (■).

TMAI- and TBAI-containing cathode cells. As can be seen, the increase in the alkyl group from methyl to butyl increases the discharge period even at relatively higher current densities. This confirms the fact that the cage-like structure of the alkyl group traps molecular iodine, reducing its activity and aiding sufficiently longer discharge periods. The internal resistance of the cells of the types II and III seems to remain almost the same even after the discharge process is completed. This can be attributed to the formation of tetra-alkyl ammonium iodide–silver iodide double salts, during discharge at the cathode–electrolyte interface which are also very highly conductive [20]. This double salt formation might also be one of the reasons for the longer discharge periods of cells II and III.

Figure 5 shows the comparative discharge efficiency between cells I, II and III. The capacities of cells I, II and III were found to be 8.5, 10.14 and 14.65 mAh, respectively, at a discharge current density of 0.25 mA cm^{-2}.

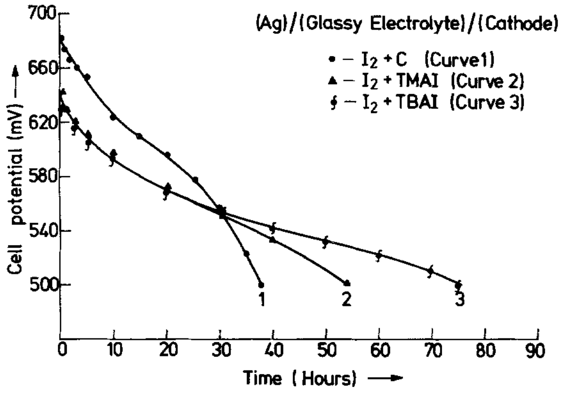

Fig. 5. The variation of cell potential with time for the amorphous electrolyte (mol %) 70AgI–20Ag_2O–10(0.8V_2O_5–0.2P_2O_5) with iodine (curve 1), TMAI (curve 2) and TBAI (curve 3) cathode materials at a discharge rate of 0.25 mA cm^{-2}.

Figure 6 indicates the variation of cell potential with discharge current density. The value of each potential was recorded 60 s after connecting each load. It can be seen that cells of the type I can be discharged only up to current densities of 1.0 mA cm^{-2}, whereas cells of the types II and III can be discharged up to 5.0 mA cm^{-2} without any serious polarization. This suggests the application of tetra-alkyl ammonium iodide-containing cathode cells to high current density discharges and longer shelf-life requirements.

As the tetra-alkyl ammonium iodides have the inherent characteristic nature of retaining molecular iodine while charging and releasing with reduced activity during discharge [21], work on the rechargeability of these cells has been undertaken.

The reversibility of the cell configuration III was tested by studying the micropolarization curves. The discharge–charge efficiency of the cell was found to be satisfactory. The discharge–charge cycle of the cell

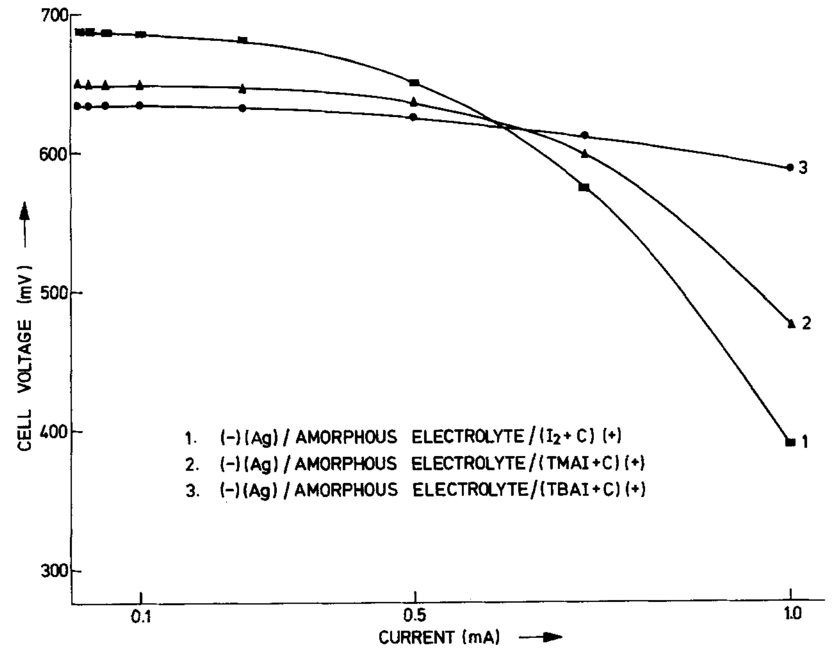

Fig. 6. The variation of cell potential with current density for the three cells with iodine (1), tetra-methyl ammonium iodide (2) and tetra-butyl ammonium iodide (3) as cathodes.

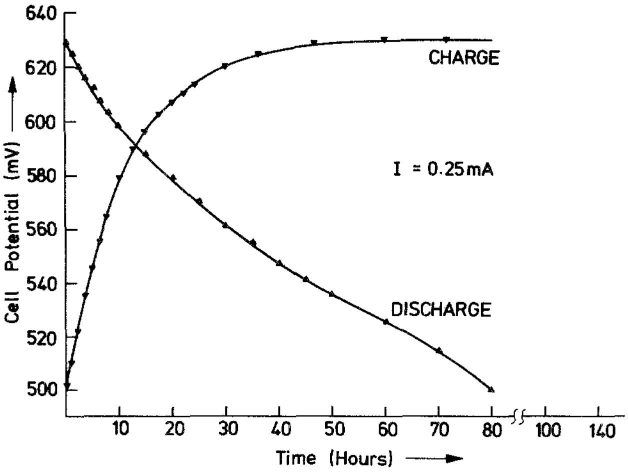

Fig. 7. The first discharge–charge cycle of the cell (Ag)/amorphous electrolyte)/(I_2 + TBAI + C) at 32° C.

shown in Fig. 7 indicates the utility of the cell as an electrical storage component in a microionic circuit for any desired time with an ability to activate the discharged cell within a short period of 5 h at a current charge rate of 0.25 mA. Hence the shelf-life of the cell is high compared to the classical elecrolyte $RbAg_4I_5$ solid state cell with I_2-Perylene complex cathode [22].

To investigate the utility of the cell in a rechargeable battery, the discharge–charge cycling was repeated 25 times at a current discharge–charge rate of 0.25 mA. The discharge–charge profile of the first cycle is shown in Fig. 7 and that of the 5th, 10th, 15th, 20th and 25th in Fig. 8. By the time the cell reaches 20 cycles, the coulombic efficiency has reduced to 40%. On disconnecting the cell and removing the positive electrode, dendritic deposition of silver was observed under a scanning electron microscope. The deposition of silver is thought to be the cause of the decrease in the discharge efficiency of the cells after 20 cycles. Also, the charging efficiency reduces by 50%, as illustrated in Fig. 8. At the 25th cycle, the cell retains a cell potential of 600 mV after 24 h, whereas it takes 12 h to obtain the same potential in the 20th cycle. This shows that both discharge and charge efficiencies reduce drastically after 25 cycles.

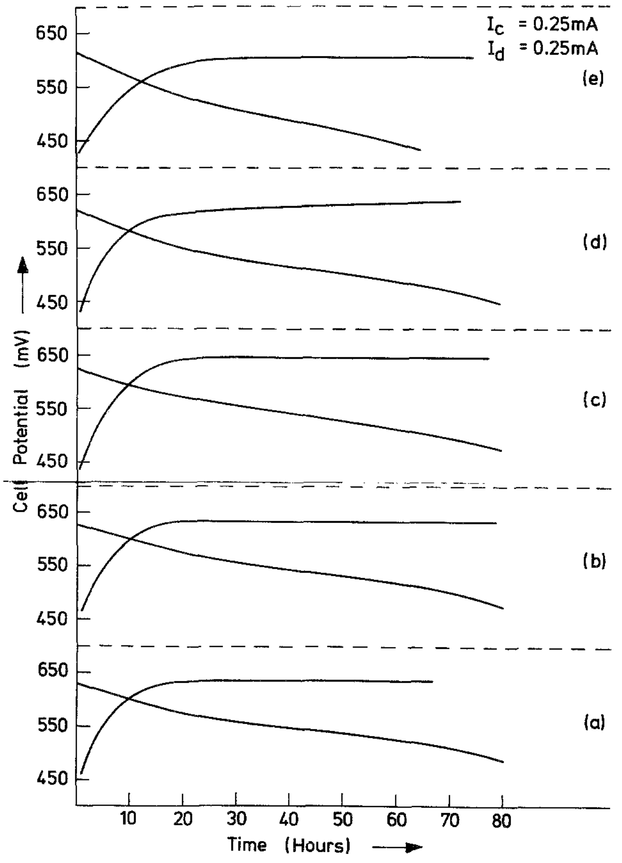

Fig. 8. Discharge–charge cycles of cell III at 5th cycle (a), 10th cycle (b), 15th cycle (c), 20th cycle (d) and 25th cycle (e) at 32° C.

The cell was subjected to deep discharge–charge cycles to confirm the dendritic deposition of silver on the negative electrode. On reaching the 10th cycle, a steep fall in the cell potential was observed in discharge and a reduction in cell potential after charging for 48 h. Hence, it can be concluded from the micropolarization curves and cyclic voltammetric studies that these cells have great potential in the development of silver rechargeable batteries for applications in micropower sources, specialized applications in space and as storage components in microionic circuits.

Acknowledgements

One of the authors (PSSNP) would like to thank the Council of Scientific and Industrial Research (CSIR), India for their financial help in the form of a senior research fellowship (SRF) and Dr G Rajendran, Electrochemistry Lab., Dept of Chemistry, I.I.T, Madras for the valuable discussions on organic cathode materials.

References

[1] J. N. Bradley and P. D. Greene, *Trans. Farad. Soc.* **63** (1967) 424.
[2] B. B. Owens and G. R. Argue, *Science* **157** (1967) 308.
[3] G. W. Mellows and D. U. Louzos, *J. Electrochem. Soc.* **118** (1971) 846.
[4] T. Takahashi, S. Ikeda and O. Yamamoto, *J. Electrochem. Soc.* **119** (1972) 477.
[5] T. Takahashi and O. Yamamoto, *Electrochim. Acta* **11** (1966) 779.
[6] C. C. Liang, J. Epstein and G. H. Boyle, *J. Electrochem. Soc.* **116** (1969) 1452.
[7] K. Hariharan, C. V. Tomy and R. Kaushik, *Bull. Electrochem.* **1** (1985) 405.
[8] B. Scrosati, F. Papeleo, G. Pistoia and M. Lazzari, *J. Electrochem. Soc.* **22** (1974) 339.
[9] G. Chiodelli, A. Magistris and A. Schiraldi, *Electrochim. Acta* **19** (1974) 655.
[10] T. Minami, K. Imazawa and M. Tanaka, *J. Non-Cryst. Solids* **42** (1980) 469.
[11] P. Sathya Sainath Prasad and S. Radhakrishna, *J. Non-Cryst. Solids* (communicated).
[12] P. Sathya Sainath Prasad and S. Radhakrishna, *J. Mat. Sci. Lett.* **7** (1988) 113.
[13] P. Sathya Sainath Prasad and S. Radhakrishna, *J. Mat. Sci.* **23** (1989) in press.
[14] P. Sathya Sainath Prasad and S. Radhakrishna, *J. Solid State Chem.* **76** (1988) 7.
[15] A. V. Joshi and J. B. Wagner, *J. Phys. Chem. Solids* **33** (1972) 205.
[16] B. B. Owens, *J. Electrochem. Soc.* **117** (1970) 1536.
[17] T. Minami, Y. Takuma and M. Tanaka, *J. Electrochem. Soc.* **124** (1977) 1659.

[18] B. Scrosati, *Appl. Chem. Biotechnol.* **21** (1977) 78.
[19] B. B. Owens, J. H. Christie and G. Trent Tiedman, *J. Electrochem. Soc.* **118** (1971) 1144.
[20] J. E. Oxley and B. B. Owens, in 'Power Sources 3' (edited by D. H. Collins), Oriel Press, Newcastle upon Tyne (1971) p. 535.
[21] M. Lazzari, B. Ribolta and F. Bonino, *J. Power Sources* **2** (1977) 389.
[22] B. Scrosati, *J. Electrochem. Soc.* **120** (1977) 78.